The Crop Journal 11 (2023) 679–691

Contents lists available at ScienceDirect

The Crop Journal

journal homepage: www.keaipublishing.com/en/journals/the-crop-journal/

Barley *FASCIATED EAR* genes determine inflorescence meristem size and yield traits

Chengyu Wang [a], Xiujunan Yang [b], Yueya Zhang [c], Chaoqun Shen [b,c], Jin Shi [c], Chongjing Xia [a], Taohong Fang [a], Qiang Tu [a], Ling Li [c], Xinli Zhou [a], Dabing Zhang [b,c], Gang Li [b,d,*]

[a] School of Life Sciences and Engineering, Southwest University of Science and Technology, Mianyang 629000, Sichuan, China
[b] School of Agriculture, Food and Wine, Waite Research Institute, The University of Adelaide, Adelaide 5005, SA, Australia
[c] School of Life Science and Biotechnology, Shanghai Jiao Tong University, Shanghai 200240, China
[d] Department of Plant Pathology, College of Plant Protection, Nanjing Agricultural University, Nanjing 210095, Jiangsu, China

ARTICLE INFO

Article history:
Received 25 June 2022
Revised 7 September 2022
Accepted 6 October 2022
Available online 25 October 2022

Keywords:
Inflorescence meristem
Yield traits
FASCIATED EAR genes
Gene expression
Barley

ABSTRACT

In flowering plants, the inflorescence meristem (IM) provides founder cells to form successive floral meristems, which are precursors of fruits and seeds. The activity and developmental progression of IM are thus critical for yield production in seed crops. In some cereals, such as rice (*Oryza sativa*) and maize (*Zea mays*), the size of undifferentiated IM, which is located at the inflorescence apex, is positively associated with yield traits such as spikelet number. However, the relationship between IM size and yield-related spike traits remains unknown in the Triticeae tribe. Here we report that IM size has a negative correlation with yield traits in barley (*Hordeum vulgare*). Three *FASCIATED EAR* (*FEA*) orthologs, *HvFEA2*, *HvFEA3*, and *HvFEA4*, regulate IM size and spike morphogenesis and ultimately affect yield traits. Three *HvFEAs* genes are highly expressed in developing spikes, and all three loss-of-function mutants exhibit enlarged IM size, shortened spikes, and reduced spikelet number, which may lead to reduced grain yield. Natural variations identified in *HvFEAs* indicate selection events during barley domestication. We further reveal that HvFEA4, as a transcription factor, potentially targets multiple pathways during reproductive development, including transcriptional control, phytohormone signaling, and redox status. The roles of barley *FEA* genes in limiting IM size and promoting spikelet formation suggest the potential of increasing yield by manipulating IM activity.

1. Introduction

Plant inflorescence structures initially derive from the inflorescence meristem (IM), a group of stem cells that are responsible for initiating lateral primordia such as those of branches and flowers [1,2]. In cereal crops, grain yield is determined mainly by the number of inflorescences per plant, kernel number per inflorescence, and kernel dimensions [3,4]. Among these factors, inflorescence architecture determines the capacity and arrangement of kernels, such as a panicle in rice, an ear in maize, and a spike in wheat (*Triticum aestivum* L.) and barley [4,5]. The phase shift from vegetative shoot apical meristem (SAM) to reproductive IM is elaborately regulated and characterized by morphological changes starting with the rapid increase of meristem size [1,4,6]. The IM then starts to initiate branch primordia or spikelet meristems, followed by the formation of spikelets and florets. The programming of IM activity varies to form varied inflorescence architectures.

Meristem size and phase transition from SAM to IM are found to be controlled by the CLAVATA (CLV) –WUSCHEL (WUS) negative feedback pathway [2,7–11]. In the dicot plant *Arabidopsis thaliana*, this pathway involves CLV3, a small peptide recognized by leucine-rich repeat receptor kinases CLV1 and CLV2, which acts to restrict the expression domain of the transcription factor gene *WUS*. WUS consummates the negative feedback loop by stimulating *CLV3* expression to maintain meristem homeostasis [1,4,10]. Any loss of function disturbing CLV–WUS loop could lead to changed IM size and activity [12–14]. Similarly, a CLV–WUS pathway underlying meristem size control and inflorescence specification has also been identified in monocot plants such as rice and maize [10]. Rice *FLORAL ORGAN NUMBER 1* (*FON1*) and *FON2*/*4* are orthologs of *CLV1* and *CLV3*, respectively [15–17]. Genetic analysis has revealed that

* Corresponding author.
E-mail address: gang.li@njau.edu.cn (G. Li).

https://doi.org/10.1016/j.cj.2022.10.001

FON1 and *FON2/4* are required for rice SAM size control, IM activity and FM formation [16]. In maize, most members of the CLV–WUS pathway have been identified by gene cloning from mutants showing the fasciated ear (FEA) phenotype. For instance, THICK TASSEL DWARF1 (TD1) and FEA2 are the closest orthologs of *Arabidopsis* CLV1 and CLV2, respectively [18–20]. ZmCLE7 (CLAVATA3/ESR-related peptide) and ZmCLE14 have been identified as potential CLV3 orthologs [21]. Loss-of-function mutants display increased IM size and produce more axillary meristems (AMs), thereby forming fasciated ears. The dominant maize mutant *Bif3* (*Barren inflorescence3*), harboring a tandemly duplicated copy of *ZmWUS1*, also shows increased meristem size, but is unique in initiating only a reduced number of AMs [22], suggesting the complex regulation of CLV–WUS pathway in inflorescence development of monocots. Similar to FEA2 in sequence, FEA3, acting as a new CLV receptor in maize, has been integrated into a regulatory model of CLV–WUS feedback [21]. The *fea3* mutant shows enlarged IMs with expanded *ZmWUS1* expression, also developing into a fasciated ear [21]. Additionally, FEA4 functions as a bZIP transcription factor that restricts meristem size by regulating the expression of genes involved in meristem determinacy, auxin signaling, and redox state, independent of the CLV pathway [23–25]. The maize *fea4* mutant exhibits enlarged meristem size and fasciated ear phenotype similar to that of *fea2* and *fea3* [23]. Together, IM maintenance and activity require multiple mechanistically regulatory networks, including CLV-dependent and -independent pathways, but these have been described in few model plants or crops.

Regulation of IM size and activity has been shown to be associated with grain or fruit production in plants [1,4]. Mutations of *Arabidopsis CLV1*, *CLV2*, and *CLV3* lead to increased numbers of flowers and floral organs [12–14]. Mutations in the tomato CLV pathway genes *SlCLV3*, *FASCIATED AND BRANCHED*, and *FASCIATED INFLORESCENCE* also cause enlarged meristems, leading to an increase in inflorescence branching [26,27]. Rice *fon2/4* mutants exhibit increased numbers of primary branches, florets, and floral organs. By contrast, overexpression of *FON2* leads to a smaller IM with reduced floral organs [16]. In maize *fea2* null mutants, owing to a compensatory reduction in kernel size, overall yield does not increase [28]. However, a weak *FEA2* allele has been found that confers higher kernel row number and yield [29]. Similarly, the weak allele of *FEA3* increases kernel row number [21]. These reports indicate that fine-tuned expression of genes in the CLV–WUS pathway functions in yield improvement of cereals, as also shown in maize and tomato by gene editing of *CLV3* genes [6,30,31]. Notably, testing of CLV–WUS components' alleles in field trials suggests that applied strategies for the basic knowledge of meristem size regulation have the potential to increase crop yields [10,29].

In Triticeae crops including wheat and barley, the spike meristem contains the undifferentiated IM at the apex and the spikelet meristems (SMs) attach to the axis without forming branches, suggesting the direct effect of IM activity on spikelet number and grain yield [4,32]. Several transcription factors have been reported to determine IM and SM identity, including MADS proteins, APETALA2 (AP2), TB1 (Teosinte Branched 1, e.g., VRS5, Six-rowed spike 5) family [33–39], showing either conserved or divergent regulatory functions. However, IM size control and its relationship with yield performance remain largely unknown. In this study, we show that barley IM size appears to be negatively correlated with yield traits of spikes. Three orthologs of maize FEAs, CLV members FEA2 and FEA3, bZIP transcriptional factor FEA4, have been identified in barley by phylogenetic analysis and our previous transcriptome data [40]. Loss of function of *HvFEA2*, *HvFEA3* or *HvFEA4* causes increased IM width but reduced spike length and spikelet number, supporting the negative correlation between IM size and yield traits. We also reveal the regulatory mechanism of HvFEA4 in developing barley IM, which potentially affects genes involved in reproduction, transcriptional activity, and hormone signaling. These findings shed light on the mechanism of meristem development involving FEA proteins in barley, giving rise to novel understandings of yield improvement in crops.

2. Materials and methods

2.1. Barley FEA identification and phylogenetic analysis

HvFEAs were identified based on maize FEA2, FEA3, and FEA4 protein sequences from previous studies [18,21,23]. NCBI (https://www.ncbi.nlm.nih.gov/) and Ensembl Plants (https://plants.ensembl.org/index.html) were used to align the protein sequences of HvFEAs and their orthologs in other plants. Sequences of barley FEAs were confirmed in the reference Morex genome database (https://webblast.ipk-gatersleben.de/barley_ibsc/) [41]. For phylogenetic analysis, FEA orthologs (with sequence identity > 60%) from other plants, including wheat, rice, and sorghum (*Sorghum bicolor*) in monocots, and tomato (*Solanum lycopersicum*), *Arabidopsis* (*Arabidopsis thaliana*), tobacco (*Nicotiana tabacum*) in eudicots, and others, were selected. A Bayesian phylogenetic tree was constructed with BEAST (version 2.3) [42] with the HKY + G (5 categories) substitution model and Yule model priors. A Markov chain Monte Carlo chain was run for 5,000,000 generations with 10% burn-in until convergence. The final phylogenetic tree was inferred by TreeAnnotator [42], and further annotated with the ggtree (version 1.16.6) package in R [43].

2.2. Plant growth conditions and generation of barley mutants

Barley plants of wild type (WT) and mutants were grown in cocopeat soil, under 15 °C in light and 10 °C in dark, with a 16 h photoperiod at 50% humidity in growth chambers. Barley cultivars used for IM size measurement and spike and seed trait investigation were grown in the field at Waite Campus (University of Adelaide, Australia) and Mianyang city (Sichuan, China).

Nicotiana benthamiana plants were grown in a greenhouse at 23 °C with a 16 h photoperiod. Plants were grown until they had six leaves with the youngest leaf over 1 cm in length. Then the leaves were infiltrated with *Agrobacterium*. Transformed plants were maintained under weak light in the greenhouse for 48 h until microscopy observation.

The barley (*Hordeum vulgare*) variety Golden Promise (GP) was used as a donor plant for creating mutants. Two target sequences in the first or second exons of *HvFEA2*, *HvFEA3*, and *HvFEA4* genes were selected [44]. A Blast search of the target sequences (including PAM, protospacer adjacent motif, NGG) was performed to test their targeting specificity in the barley genome using the IPK database (https://webblast.ipk-gatersleben.de/barley_ibsc/). Two target sites of *HvFEA* genes were sequenced in GP, and all showed 100% identity with the reference genome (Morex variety). SgRNA-T1 was driven by the rice promoter *OsU6a* and sgRNA-T2 was driven by the rice promoter *OsU6b* [44]. SgRNA expression cassettes of *OsU6a-sgRNA-T1* and *OsU6b-sgRNA-T2* were amplified from pYLsgRNA-OsU6a and pYLsgRNA-OsU6b plasmids using Phusion High-Fidelity DNA Polymerase (New England BioLabs) and cloned into a binary vector, pYLCRISPR/Cac9P_{ubi}-H using *Bsa*I sites as described [44]. Primers used for CRISPR/Cas9 constructs are listed in Table S1.

All constructs were transformed into *Agrobacterium tumefaciens* AGL1, and tissue transformation was performed using immature embryos of GP plants as previously described [45]. At least 30 T_0 transgenic plants from each transformation were obtained. Individual T_0 plants carrying biallelic or homozygous mutations were

identified by genotyping using a Phire Plant Direct PCR Kit (Thermo Fisher Scientific) and Sanger sequencing.

2.3. Phenotyping and scanning electron microscopy (SEM)

Barley spikes and grains were photographed with a Nikon D5600 digital camera. Inflorescence meristems in Golden Promise, *hvfea2*, *hvfea3*, and *hvfea4* mutants, and selected barley cultivars were photographed under a stereomicroscope (Leica Microsytems Ltd. DFC450) with a digital camera, and IM width (apical undifferentiated region) at W2.0 stage was measured with ImageJ software (https://imagej.net/) as previously described [21,46].

For SEM, spike meristems of different developmental stages from *hvfea2*, *hvfea3*, *hvfea4*, and GP plants were prefixed with 2.5% glutaraldehyde in phosphate buffer (pH 7.0) at 4 °C overnight. Subsequent treatments followed Li et al. [37]. Samples were observed with a scanning electron microscope (SEM, Hitachi TM-100, Hitachi, Japan) as previously described [47].

2.4. RNA extraction and RT–qPCR

For tissue-specific expression, spike meristems (Waddington stages W2.0, W3.5, W5.0, W7.0 and W9) and barley tissues: 14-day-old young root and young stem, mature leaf, flag leaf, and spikelets, were collected from the wild-type barley plant. For RNA-seq validation, several stages of spike meristems were collected from WT (GP) and *fea4* mutants. Total RNA was extracted using TRIzol reagent (Life Technologies). 1.5 μg of total RNA was incubated with 2 μL 5× gDNA Clean Buffer and 1 μL gDNA clean Reagent (*Evo* M−MLV RT Kit with gDNA Clean for qPCR II AG11711, Accurate Biology) at 42 °C for 2 min. First-strand cDNA was generated using 1 μL *Evo* M−MLV RTase Enzyme Mix and RT Primer Mix (*Evo* M−MLV RT Kit), according to the manufacturer's instructions. cDNA was used as a template for real-time RT-qPCR with a CFX96 Optics Module (BIO-RAD) machine. For reverse transcription quantitative PCR (RT-qPCR) program, DNA was denatured at 95 °C for 10 min, followed by 45 cycles at 95 °C for 10 s, 56 °C for 15 s, and 72 °C for 15 s. Gene expression was normalized to the expression levels of the housekeeping gene *HvActin7*. Primer sequences are listed in Table S1.

2.5. In situ mRNA hybridization

Spike meristems from WT plants at stages W2.0 and W3.5 were collected and fixed in FAA (5% acetic acid, 50% ethanol, and 3.7% formaldehyde in water) for 16 h at 4 °C. After dehydration in an ethanol series, tissues were embedded in Paraplast Plus (Oxford Labware) and sectioned to 8-mm thickness with a rotary microtome (YL3-A, Shanghai Instrument Factory). Specific fragments of the coding sequences, 305 bp from HvFEA2 cDNA (645–1551 bp), 289 bp from HvFEA3 cDNA (18–507 bp) and 248 bp from HvFEA4 cDNA (131–981 bp), were amplified by PCR using specific primers fused with the T7 promoter (the primers are listed in Table S1). Digoxigenin-labeled antisense and sense probes were synthesized using primers incorporating the T7 polymerase binding site at the 5′ end using an *in vitro* transcription kit (Roche) according to the manufacturer's instructions. *In situ* hybridization assays were performed as previously described [48]. Hybridization with 1.5 ng μL^{-1} digoxigenin-labeled RNA probes, post-hybridization washes, and immunodetection were performed. The slides were incubated with diluted (1:1000) antibody conjugate (anti-digoxigenin-AP; Roche; catalog number, 11093274910) in BSA wash solution and then washed in BSA wash solution (3 × 15 min). Images were acquired with an optical microscope (Olympus Nikon E600). The empty slide background was color-matched in Photoshop (Adobe) for comparison among slides.

2.6. Protein subcellular localization

To observe protein localization in *N. benthamiana* leaf epidermal cells, the full-length sequences of *HvFEA2*, *HvFEA3* and *HvFEA4* fused *eGFP* (enhanced green fluorescent protein) tag, were inserted into pCAMBIA1301 vector with *35S* promoter by *Nco* I and *Spe* I sites using In-Fusion cloning (Clontech). Free GFP and a fragment encoding nuclear localization signal (NLS) fused with mCherry were cloned in the same vector driven by the 35S promoter using *Spe* I and *BstE* II sites, serving as controls. Constructs and primers are listed in Table S1. Transient expression of proteins in *N. benthamiana* leaf epidermal cells was performed as previously described [49]. All constructs were transformed into *Agrobacterium* cells (GV3101). Overnight *Agrobacterium* cultures were collected by centrifugation, re-suspended in Murashige and Skoog liquid medium (pH 5.8) to OD_{600} = 0.6, and incubated at room temperature for 2–3 h after addition of 2-[*N*-morpholino] ethanesulfonic acid of 10 mmol L^{-1} final concentration, pH 5.6) and acetosyringone of 200 μmol L^{-1} final concentration. For co-expression assay of HvFEA4 and NLS, two *A. tumefaciens* strains were mixed in the ratio 1:1. The mixture was infiltrated into young *N. benthamiana* leaves and the plants were grown for about 48 h. Leaf samples were collected for microscopic observation.

Images were captured with a confocal laser scanning microscope (Leica TCS SP5). Fluorescence signals for eGFP (excitation, 488 nm; emission, 500–530 nm; 15% power) and mCherry (excitation, 561 nm; emission, 575–615 nm; 15% power) were detected with a 20× objective.

2.7. RNA-seq library preparation and data analysis

Inflorescence samples of wild-type (GP) and *hvfea4* plants were collected at W2.0 and W3.5. Total RNA was extracted from 15 to 20 spikes for each of three biological replicates using TRIzol (Invitrogen) and purified using a RNeasy Micro Kit (Qiagen) following the manufacturer's instructions. RNA quality and integrity were assessed on an Agilent 2200 TapeStation. Library preparation was performed using 1 μg of total RNA (with RNA integrity number > 8) using the TruSeq RNA Library Preparation Kit v.2 (Illumina, RS-122–2101 and RS-122–2001), following the manufacturer's instructions. The libraries were sequenced using paired-end sequencing of 250–300-bp fragments on a HiSeq4000 at QL-bio (Beijing, China).

The quality of raw sequencing reads for all samples was examined using FastQC (version 0.11.4; https://www.bioinformatics.babraham.ac.uk/projects/fastqc/). Reads with adaptors and of low quality (> 20% bases with quality score < 30) were removed using the BWA algorithm, and reads composed of > 5% unknown bases (labeled N) were discarded. Fragments per kilobase per million reads (FPKM) were normalized by genome-wide coverage. Clean reads were mapped to the barley reference genome (GCA_004114815.1) using HISAT2 aligner (version 2.0.0) with default parameters except that "—dta" was set. Alignment in SAM format was converted to BAM using SAMtools (version 0.1.20) [50]. Correlation between replicates was evaluated using the "multiBamSummary" module in deeptools (version 3.5.1) [51]. FPKM was normalized with HTSeq (version 0.11.2). DEGs (Differentially expressed genes) were identified using the R package EmpiRes (https://www.bio.ifi.lmu.de/software/empires/index.html) [52]. DEGs were identified and annotated based on GCA_004114815.1 annotation, as well as using BLASTx alignments against a rice protein database (MSU7_peptide; https://rice.plantbiology.msu.edu/). Heatmaps were created from DEGs using FPKM (value to ClustVis; https://biit.cs.ut.ee/clustvis/).

Venn diagrams were created from the DEGs described above, GO (Gene ontology) analysis was performed using barley

gene-to-GO associations captured from AgriGO2 (https://systemsbiology.cau.edu.cn/agriGOv2/). AgriGO2 was also used for GO classification analysis and identification of pathways of stage-specific genes. The R package ggplot2 was applied to GO enrichment analysis for DEGs [53,54].

Proteins encoded by DEGs at W2.0 from RNA-seq result were used to construct a protein–protein interaction (PPI) network. For data preparation, up- and downregulated DEGs were divided into two groups. Based on the annotation of barley genes, the symbols of these proteins were named according to orthologs from other plants. The sequences of the proteins were extracted from the barley genome database Ensembl Plants (https://plants.ensembl.org/index.html). The gene symbol with its sequence were input into the online network STRING for PPI analysis. The STRING Interactome (https://cn.string-db.org/) was selected with medium (400) to high (1000) confidence score. The confidence score cutoff was set as 900 for the analysis. The degree of each node was calculated based on the number of its connections to other nodes. The results were loaded into Cytoscape (version 2.5) software [55] to generate the final models.

2.8. Natural variation analysis

The query CDS (coding sequence) of *HvFEA2*, *HvFEA3*, and *HvFEA4* were defined from GP and 18 other varieties, including 9 two-rowed and 7 six-rowed barley, and two with other row types, representing the genetic diversity of 19,778 domesticated varieties of barley [56]. Allele investigation was based on a recent barley pan-genome study (https://galaxy-web.ipk-gatersleben.de/) [57]. Single-nucleotide polymorphisms among them were compiled for variation analysis. NovoPro (https://www.novopro.cn/tools/translate.html) was used for DNA translation. SnapGene (version 6.0.2) was used for amino acid alignment.

2.9. Yield traits of barley varieties

For yield trait investigation of barley varieties, plants were cultivated in the same field. Spikelet number was recorded at heading stage and grain number and other traits were recorded after harvesting. Grain length and width were measured with a vernier caliper. Grains and spikes were photographed with a Fujifilm X-T 200 digital camera. All measurements were performed on at least twenty samples.

2.10. Quantification and statistical analysis

All experiments were conducted with technical and biological replicates with sample sizes estimated on the basis of our previous experience. No statistical methods were used to predetermine sample size. The experiments were not randomized, and the investigators were not blinded to allocation during the experiments and outcome assessment. All experiments were replicated independently at least once, as indicated in each figure. Statistical analyses of all box and bar graphs were performed using GraphPad Prism 8.0.2 (https://www.graphpad.com/scientific-software/prism/) or Microsoft Excel 2016. Details of statistical approaches are found in figures or figure legends.

3. Results

3.1. Barley inflorescence meristem size has a negative correlation with yield traits

A general model from rice and maize studies indicates that an enlarged IM can increase its capacity of axillary meristems (such as branch meristems in rice and spikelet pair meristems in maize), leading to higher seed number [2,11,22]. These findings suggest that IM size is positively associated with yield expressed as kernel number. To test this trend in barley, we dissected young developing spikes (meristem primordia, Waddington stage 2.0 [58]) from a group of 100 cultivars, including 90 two-rowed and 10 six-rowed types, and measured the width of the inflorescence meristem (IM, undifferentiated region at the apex of the spike meristem) (Fig. 1A–C). The mean IM diameter varied among cultivars, from 85.84 μm to 134.94 μm (Table S2). We also investigated the yield-related spike traits in these barley cultivars, ranging from 19 to 40 spikelets per spike, 15 to 37 seeds (two-rowed) or 54 to 90 seeds (six-rowed) per spike, and 5.3 cm to 14.3 cm in spike length (Table S2), respectively. Surprisingly, we found a significant negative correlation between IM size and spike/yield traits in both two-rowed and six-rowed varieties. The Pearson correlations between IM diameter and spikelet number, seed number, and spike length ranged from −0.303 to −0.865 (Fig. 1A, B; Table S2). A two-rowed barley cultivar, ISBYT-LRA-M−089, had a smaller IM width, but developed a longer spike bearing more spikelets/seeds than did medium-sized Triumph and large-sized ND11231-12 (Fig. 1C, D). Thus, a larger inflorescence meristem appears to be able to impair the further differentiation of spikelet meristem and spike elongation and may eventually repress the yield in barley.

3.2. Identification of FEA orthologs in barley

In maize, three key genes, *FEA2*, *FEA3*, and *FEA4*, have been reported to influence meristem size and regulate ear architecture [21,23,28]. To identify their orthologs in barley, we collected the amino acid sequences of maize FEA2 (NP_001105662.1), FEA3 (ONM30618.1), and FEA4 (NP_001308277.1) from GenBank (https://www.ncbi.nlm.nih.gov/genbank/). BlastP was performed in the barley Morex genome database IPK Gatersleben. HORVU6Hr1G054820, HORVU3Hr1G013160, and HORVU7Hr1G042170, named HvFEA2, HvFEA3, and HvFEA4, were recognized as the closest orthologs with maize FEAs (Fig. S1).

Phylogenetic trees were constructed to investigate evolutionary relationships in each FEA family (Fig. S1). HvFEA2 and HvFEA3 were predicted to be leucine-rich repeat receptor proteins and HvFEA4 shared a common feature with TGACG-BINDING FACTOR (TGA)-class bZIP proteins. HvFEA2 was grouped with ZmFEA2 and other FEA2-like orthologs from grasses, but not with dicot clades like *Arabidopsis* CLV2. Notably, some FEA2-like members from monocots, such as *Ensete ventricosum* and *Musa acuminata*, were in the same clade with dicots (Fig. S1). FEA3 and FEA4 members were clearly divided into two clades: monocots and eudicots. Multiple members of FEA3-like and FEA4-like were identified in most species, but only one was found in barley (Fig. S1). Within the grass family, HvFEA2, HvFEA3, and HvFEA4 showed more similarity to their orthologs in wheat, *Brachypodium* (*Brachypodium distachyon*), and rice, than to those in maize and other monocot plants (Fig. S1). Further, FEA2, FEA3, and FEA4 members in barley, rice, wheat, and maize harbored conserved domains within these three families: multiple leucine-rich repeat domains in FEA2 and FEA3, transmembrane region in FEA3, and bZIP domain in FEA4 (Fig. S2A–C). Full-length amino acid alignment showed that HvFEA2, HvFEA3, and HvFEA4 had high sequence similarities with their orthologs in rice, wheat, and maize, including the key motifs, sharing 68.24%–96.22% identity (Fig. S3). These results indicate that HvFEA2 (HORVU6Hr1G054820), HvFEA3 (HORVU3Hr1G013160) and HvFEA4 (HORVU7Hr1G042170) are

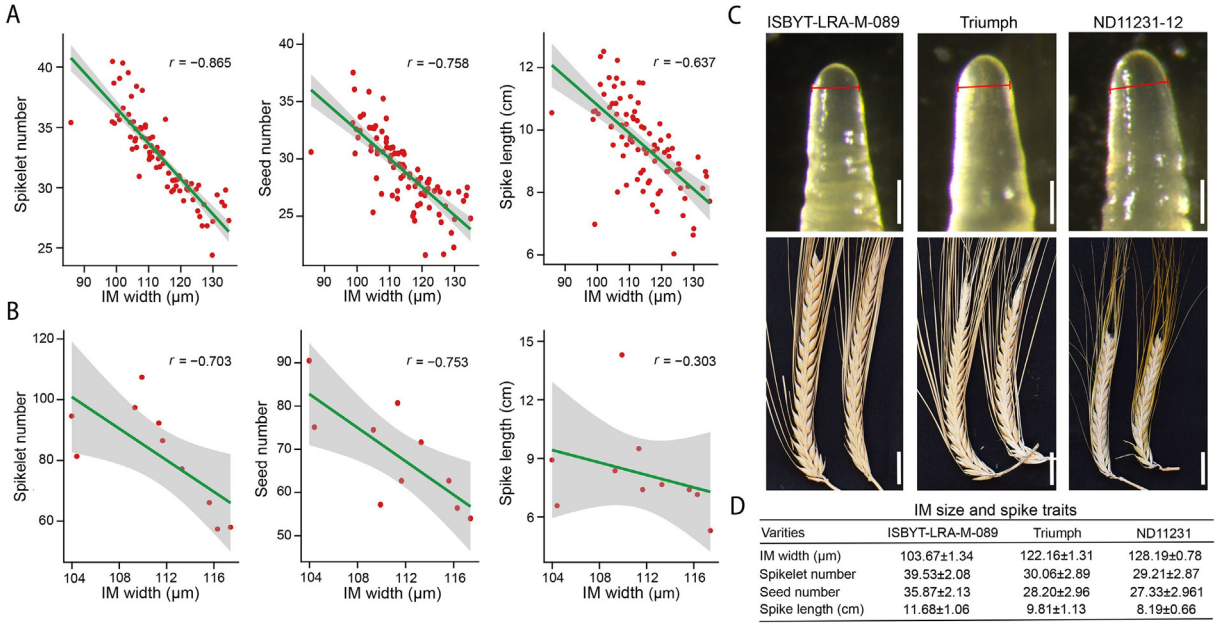

Fig. 1. Negative correlation between IM size and yield traits in barley spikes. (A, B) Correlations between inflorescence meristem (IM) size and spikelet number or seed number or spike length among 90 two-rowed (A) and 10 six-rowed (B) barley varieties. The *r* values indicate Pearson correlation. (C) Images represent the IM and mature spike of selected two-rowed barley varieties, ISBYT-LRA-M−089, Triumph and ND11231-12. Scale bars, 100 μm in IM panels and 2 cm in spike panels. (D) Average value of IM width and spike traits in ISBYT-LRA-M−089, Triumph and ND11231-12 varieties. Values of IM width and spike traits (A, B, and D) were recorded for at least 15 independent samples of each set.

candidates for barley orthologs of maize FEA2, FEA3, and FEA4, respectively.

3.3. HvFEA genes are highly expressed in barley spike

To better understand the molecular characterizations of *HvFEA2*, *HvFEA3*, and *HvFEA4*, we first investigated their expression patterns in developing barley spikes from Waddington stage 2.0 (W2.0) to W9.0 (before pollination) using RT-qPCR. All three genes showed active expression in all stages, except for *HvFEA4* at W9.0 (Fig. 2A), consistent with our previous RNA-seq experiment [40]. This finding showed that these genes are stably expressed at early stages of inflorescence development. We also detected transcripts of three *FEAs* in other tissues. In addition to florets, barley *FEAs* showed high expression in young roots, suggesting their potential roles in vegetative development (Fig. 2A). Moreover, *in situ* hybridization analysis of *HvFEA2*, *HvFEA3*, and *HvFEA4* showed similar expression features at spikelet meristems of stage W2.0 and W3.5 (awn primordium), but different expression in the undifferentiated IM regions (Fig. 2B). *HvFEA2* transcripts accumulated throughout the whole spike meristem region, and *HvFEA4* showed a moderate expression level in spike meristem but high at the apex of IM, while *HvFEA3* was barely detected at the IM (Fig. 2B), suggesting common and differentiated roles of *HvFEAs* during spike development.

Next, we examined the subcellular localization of HvFEA2, HvFEA3, and HvFEA4 fused with an eGFP tag and transiently expressed in *N. benthamiana* leaf epidermal cells driven by the CaMV35S promoter (*35S$_{pro}$::HvFEA2-GFP*, *35S$_{pro}$::HvFEA3-GFP* and *35S$_{pro}$::HvFEA4-GFP*) (Fig. 2C). Confocal microscopy showed that HvFEA2-GFP and HvFEA3-GFP were localized mainly at the plasma membrane (Fig. 2C), in agreement with their predicted function as receptors. HvFEA4-GFP was detected exclusively in the nucleus, overlapping with the NLS marker protein (NLS-mCherry) (Fig. 2C), indicating of its function as a transcription factor.

3.4. Loss of function of HvFEAs leads to enlarged IM size and reduced SM formation

To functionally characterize the roles of FEAs in barley inflorescence development, we used a monocot-optimized CRISPR/Cas9 system [44] to engineer *HvFEA2*, *HvFEA3*, and *HvFEA4* in the barley variety Golden Promise for generating individual loss-of-function mutants. Two targets from each gene were selected for sgRNA (single guide RNA) (Fig. S4A–C). Genotyping of transgenic lines revealed the occurrence of insertion and/or deletion mutations at both target sites, leading to premature stop codons or changed amino acid sequences of HvFEA2, HvFEA3, and HvFEA4 in transgenic plants. At least five independent homozygous mutants of *hvfea2*, *hvfea3,* and *hvfea4* were obtained from the T_0 generation (Fig. S4A–C). Among the mutants, hvfea3 showed a plant architecture similar to that of the WT, but hvfea2 and hvfea4 displayed a modest dwarfism phenotype (Fig. S4D), indicating their divergent roles in plant development.

Next, we compared the widths of IMs in *hvfea2*, *hvfea3*, and *hvfea4* mutants with that of the WT. IMs from mutants were 6.23%–12.61% larger than those of wild-type plants (mean diameter 124.27 ± 5.76 μm in *hvfea2*, 123.48 ± 3.96 μm in *hvfea3*, 130. 90 ± 9.47 μm in *hvfea4*, vs. 116.24 ± 9.13 μm in WT) (Fig. 3A, B). At stage W3.5, WT spikes developed spikelet meristems (SM) containing the central spikelet and the lateral spikelets, and *hvfea2* and *hvfea3* showed similar patterning of SM on the axis with WT, according to SEM and stereomicroscopic observation (Fig. 3C). However, some *hvfea4* SMs showed an irregular arrangement on the axis, with several ectopic spikelets forming between two SMs (Fig. 3C), indicating its specific roles of *HvFEA4* in barley spikelet development. To validate the effects of IM size on spikelet number, we compared the SM number at W2.0 and W3.5 between WT and mutants. *fea* plants developed fewer SMs at both stages, especially at W3.5 (average 32 in *hvfea2*, 33 in *hvfea3*, 30 in *hvfea4*, vs 40 in WT) (Fig. 3D), verifying the negative relationship between IM size and spikelet number in barley cultivars (Fig. 1). These results

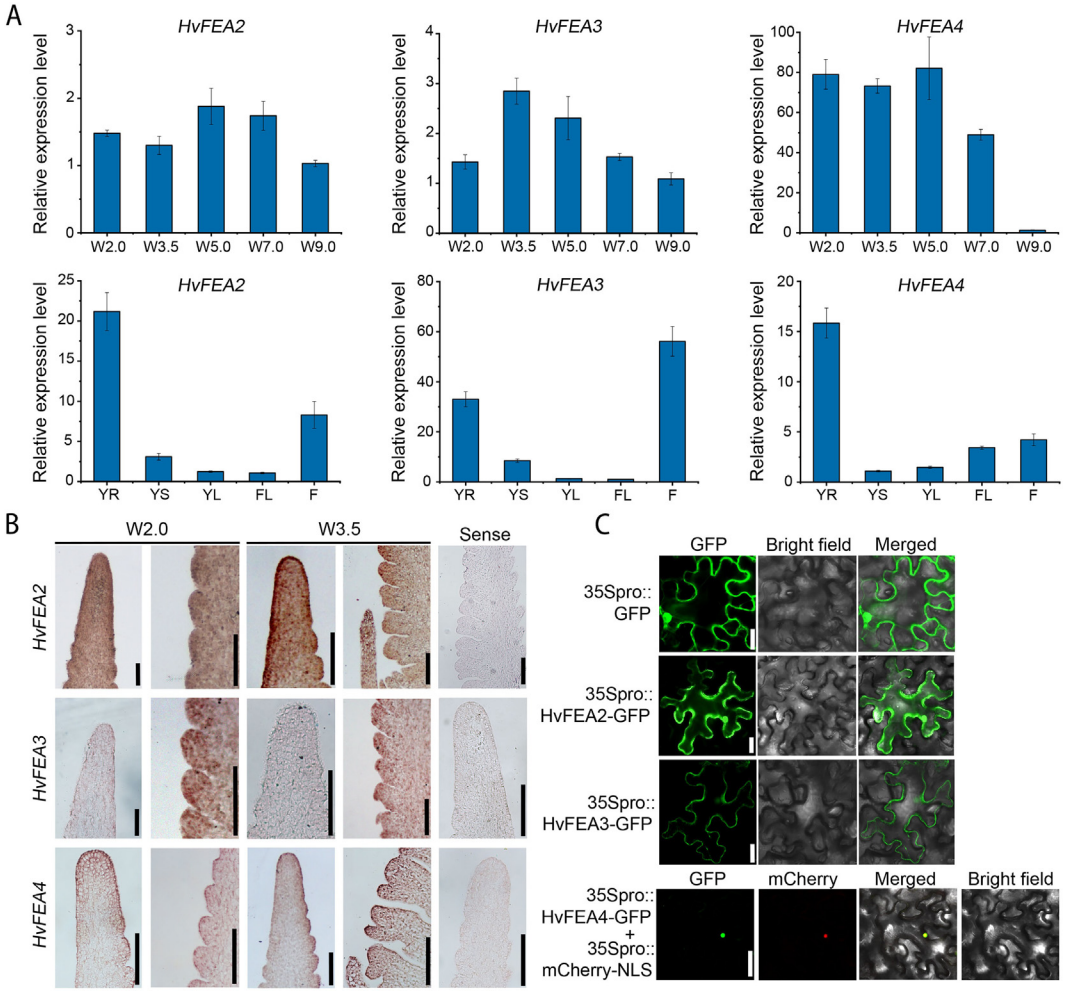

Fig. 2. Molecular characterization of barley *FEA* genes. (A) Relative expression of *HvFEA2*, *HvFEA3* and *HvFEA4* genes in developing spike meristem (Waddington stages W2.0, W3.5, W5.0, W7.0, and W9) and barley tissues. YR, young root (14 days old); YS, young stem (14 days old); YL, young leaf; FL, flag leaf; F, floret. Values are mean ± s.d. from three biological replicates. (B) *In situ* hybridization showing the expression of *HvFEA2*, *HvFEA3* and *HvFEA4* in the top apex of inflorescence meristem and spikelet meristem at W2.0 and W3.5. Scale bars, 100 μm. (C) Subcellular localization of HvFEA2, HvFEA3, and HvFEA4 proteins in *N. benthamiana* leaf epidermal cells. All proteins fused to GFP tags were transiently expressed under the control of the 35S promoter. HvFEA4-GFP was co-expressed with an NLS (Nuclear localization signal) marker protein fused with a mCherry tag. Empty GFP (*35Spro::GFP*) served as control. Scale bars, 30 μm. All experiments were repeated three times independently with similar results.

indicate that *HvFEA2*, *HvFEA3*, and *HvFEA4* function in spike meristem progression and that loss of function of *FEAs* increases IM size but reduces spikelet number.

3.5. HvFEAs regulate barley spike morphology and yield traits

Further, we compared the spike architectures of the *hvfea2*, *hvfea3*, and *hvfea4* mutants with WT at heading stage. All three mutants showed reduced spike length, especially *hvfea2* (Fig. 4A–C), but the spikelet shape was normal. The spikelet numbers per spike of the three mutants were significantly lower than that of WT (Student's *t*-test $P < 0.01$) (Fig. 4A–C), ultimately leading to reduced seed numbers per plant in *hvfea2*, *hvfea3*, and *hvfea4* mutants, compared with WT (Fig. 4D). Besides, *hvfea4* mutants generated 1–2 ectopic spikelets from the axis with no paired spikelet, and some spikelets were oppositely arranged in the axis, in contrast with the alternate pattern in WT (Fig. 4A, B). These phenotypes are consistent with the observation of spike meristems at earlier stages (Fig. 3). Compared with WT, *hvfea2* and *hvfea3*, but not *hvfea4* mutants, showed reduced grain length (Fig. 4E, F). The grain width and weight of these three mutants were similar to those of WT (Fig. 4F). These findings indicate that *HvFEA2*, *HvFEA3*, and *HvFEA4* regulate inflorescence meristem to determine spike morphology, and that *HvFEA2* and *HvFEA3* may also affect reproduction after pollination. Thus, loss of function of *HvFEAs* leads to reduced spike length and spikelet number, once again verifying the negative effects of IM size on barley yield traits.

3.6. Variations of HvFEAs in barley accessions

To test whether *HvFEA* genes were involved in varietal selection during barley domestication, we next analyzed the natural variations of these three genes in 19 barley accessions that were sequenced in a previous pan-genome study [57]. These *HvFEAs* exhibited multiple variations that were independent of row type. Except for only one variety showing no variation compared with Golden Promise (GP), 7 of 18 accessions displayed nucleotide changes in all *HvFEA* genes (Fig. 5A). Overall, *HvFEA2* had a lower variation frequency of 36.8%, while *HvFEA3* and *HvFEA4* showed 78.9% and 73.6%, respectively (Fig. 5A), indicating that *HvFEA2* has a more conserved sequence than *HvFEA3* and *HvFEA4* during domestication. By comparing the amino acid sequences, we demonstrated that these alleles did not lead to premature termination or frame-shifting (Fig. 5B; Table S3), but only amino acid

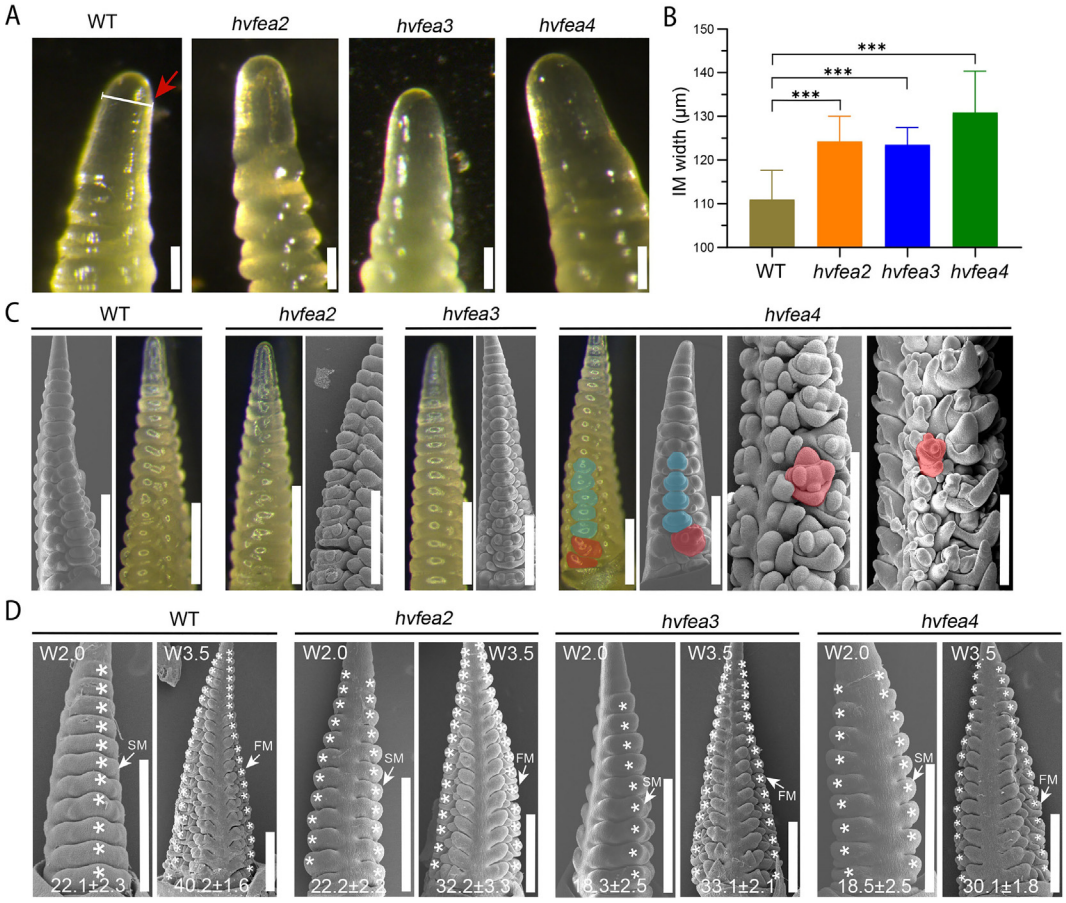

Fig. 3. Barley *FEA* genes regulate development of the spike meristem. (A) Images represent the inflorescence meristem of WT (GP background), *hvfea2*, *hvfea3*, and *hvfea4* mutants at W2.0 stage. Red arrow and white line indicate position and scale of IM. Scale bars, 100 μm. (B) Quantification of IM width in WT, *hvfea2*, *hvfea3*, and *hvfea4* mutants at W2.0 stage. Student's *t*-test was applied to compare WT with each *hvfea* mutant: ***, $P < 0.001$. (C) Images represent the spikelet meristem (SM) of WT, *hvfea2*, *hvfea3*, and *hvfea4* at W3.5 stage. Blue shading indicates normal and red shading indicates ectopic spikelet SM at *hvfea4*. Scale bars, 500 μm. (D) Scanning electron microscopy of spike meristem morphology in WT, *hvfea2*, *hvfea3*, and *hvfea4* plants. White arrows and asterisks indicate SM, and average SM numbers are shown at the bottom. Scale bars, 500 μm.

substitution or insertions occurring at specific positions. For example, HvFEA2 harbored mutations mainly at positions 422 (A to T) and 609 (R to Q) (Table S3). HvFEA3 showed many changes, and 15 of 18 varieties showed mutations in amino acids within the region 74–444 (Fig. 5A; Table S3). Variations of HvFEA4 occurred mainly from positions 96–192. Most varieties showed an insertion at 142/143 (GT insertion) and substitution at 192 (S to A), suggesting that these two types were selected at early domestication stage. Additionally, position 123 of HvFEA4 in GP was different from those in the other 19 varieties, suggesting that this variation may occur only in the GP lineage (Fig. 5B). Our findings reveal active variation of *HvFEAs* during barley domestication, which may contribute to various IM size and spike traits among barley accessions.

3.7. HvFEA4 regulates multiple biological processes during inflorescence development

FEA4 encodes a putative bZIP transcription factor of TGA family that is known to regulate a downstream network during maize ear development [23–25]. We compared the transcriptomes in WT and *hvfea4* at two key stages, W2.0 and W3.5, to identify regulatory roles of HvFEA4. In total, 1063 DEGs were identified, including 77 DEGs overlapping in the W2.0 and W3.5 stages (Fig. 6A, B; Tables S4–S6). More DEGs were up-regulated in the *hvfea4* mutant, particularly at W2.0 stage (Fig. 6A, B), suggesting that HvFEA4 likely represses downstream gene expression. GO term analysis showed that "transcriptional regulation", "reproductive process" and "oxidation–reduction process" were significantly enriched in the DEGs at both stages of spike development (Fig. 6C; Tables S5, S6).

An expression heatmap showed that a large number of receptor kinase and transcription factor genes were up-regulated in *hvfea4* mutants (Fig. 6A, D; Table S7). In particular, transcription factors such as bHLHs, MYBs and WRKYs were up-regulated at W2.0 but not W3.5 (Fig. S5; Table S8), while kinase genes were misregulated at both stages (Fig. S6; Table S8). Among the DEGs, *TAWAWA* (*TAW*)-like genes, orthologs of a critical inflorescence regulator *TAW* in rice [59], were dramatically up-regulated in the mutant (Fig. 6D). MADS-box genes, *HvMADS1*, *HvMADS5* and *HvMADS16* showed reduced expression, but spike meristem phase transit repressor SVP-like (SHORT VEGETATIVE PHASE) genes *HvMDS47* and *HvMADS55* [38,39], were up-regulated at W2.0 of *hvfea4* spikes (Fig. 6D; Table S7), suggesting that HvFEA4 likely promotes the barley spike meristem phase transition by repressing SVPs. We also examined some known regulators of barley spike meristem [4], including TCP transcription factors, *TFL1*-like (*TERMINAL FLOWER 1*) gene, *ASP1* (*ABERRANT SPIKELET AND PANICLE1*) [60], and *VRS5*, were misregulated in the *hvfea4* mutant (Fig. 6D; Table S7). Consistent with the RNA-seq results, our RT-qPCR assays confirmed the differential expression of these genes (Figs. 7A, B, S7). Our findings suggest that HvHEA4 orchestrates gene expression in barley spike development.

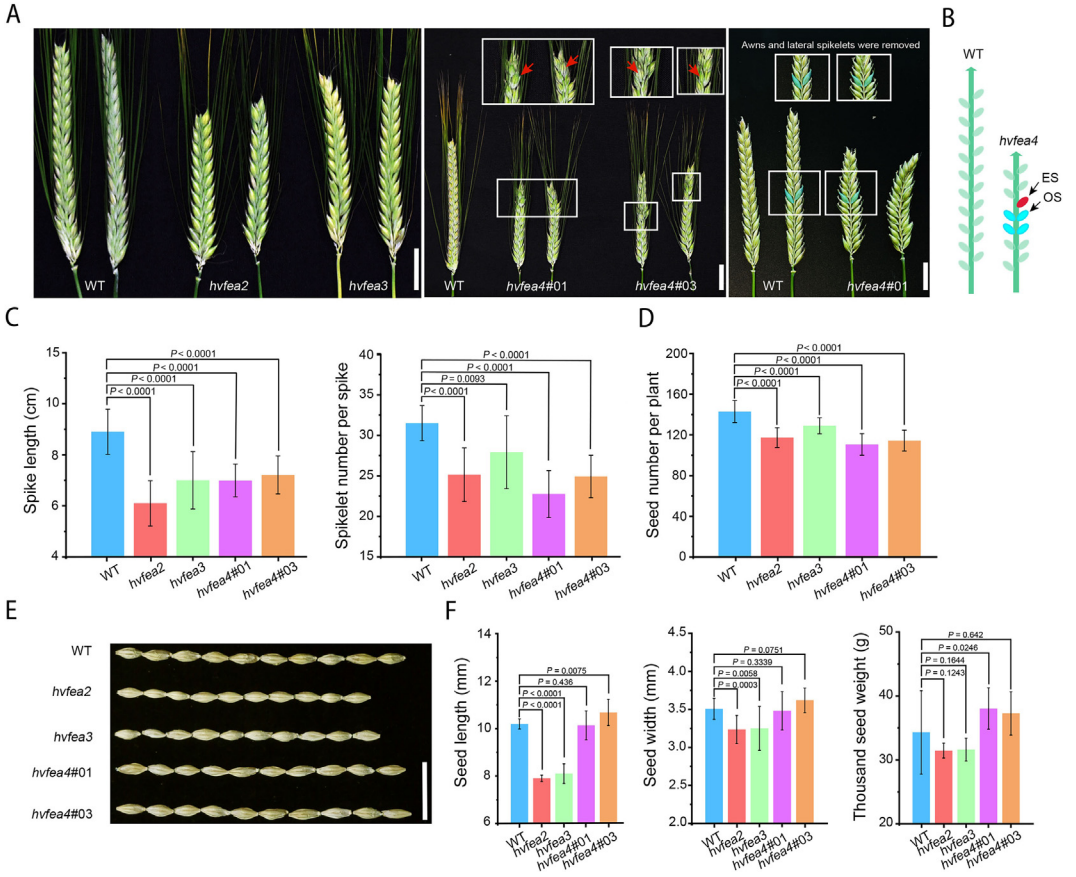

Fig. 4. Loss of function of *hvfea* genes lead to the abnormal spike morphology and poor yield traits. (A) Inflorescence phenotypes of *hvfea2*, *hvfea3*, and *hvfea4* mutants at grain-filling stage. Red arrows indicate ectopic spikelets in *hvfea4* mutants. Blue shading indicates opposite spikelet arrangement. Scale bars, 2 cm. (B) Schematic of *hvfea4* inflorescence architecture showing an ectopic spikelet (ES, indicated by red) and an opposite spikelet (OS, indicated by blue). (C) Spike traits of *hvfea2*, *hvfea3*, and *hvfea4* mutants. n = 20. (D) Average seed number per plant of *hvfea2*, *hvfea3*, and *hvfea4* mutants (n = 20 plants of each genotype). (E) Seeds of *hvfea2*, *hvfea3*, and *hvfea4* mutants. Scale bars, 2 cm. (F) Yield traits of *hvfea2*, *hvfea3*, and *hvfea4* mutants. Student's t-test was used to compare WT with each *hvfea* mutant (P-values).

In addition, we investigated the DEGs from hormonal pathways, such as auxin, gibberellin (GA) and cytokinin (CK), which are essential for meristem function [61]. Auxin signaling-associated genes, *SAURs* (*Small Auxin Up RNA*), and *CYBDOM1*-like (*Cytochrome b561 and DOMON Domain-containing Protein*) [62], showed opposite trends of change between W2.0 and W3.5, but genes responding to GA and CK were generally down-regulated in *hvfea4* (Fig. S8A, B; Table S8), suggesting the dynamic and complex influences of HvFEA4 on hormone pathways.

3.8. Regulatory networks of HvFEA4 in barley inflorescence development

Next, we constructed a hypothetical PPI model for the potential downstream proteins of HvFEA4. A network for proteins encoded by up-regulated DEGs at W2.0 showed that several reproductive regulators, transcription factors, and kinases may collaboratively contribute to barley spike meristem development (Fig. S9A). The main net includes two central proteins participating in oxidation reactions, AOS-like (Allene Oxide Synthase) and CYP85A3-like (Cytochrome P450 Superfamily Protein) [63]. The redox status might modify functions of other key proteins, such as TAW1-like, AP2-like and RINs (RNI-like Superfamily Protein) (Fig. S9A). Supportively, we selected DEGs of oxidation reactions for heatmap analysis, showing that most of them were up-regulated in *hvfea4* mutant (Fig. S10), suggesting that loss of function of *HvFEA4* likely leads to fluctuating redox activities in spikes. The PPI network also helped explain down-regulated inflorescence regulators (Fig. S9B). HvFEA4 may interact with MADS58 to connect with other key regulators, including known VRS5 and MADS1, and the absence of HvFEA4 may cause the inactivation of the whole network.

In maize, FEA4 functions in inflorescence meristem independently of CLV signaling [23]. Similarly, in barley, *HvFEA2* expression showed no difference between the WT and *hvfea4* mutant, and *HvFEA3* was slightly down-regulated in *hvfea4* mutant (Fig. S11A). Considering that some homologs of CLV–WUS pathway members also showed changed expression in *hvfea4* mutant (Fig. 6D), we validated the expression level of potential master regulator, *WUSCHEL*-like (*WUS*-like, HORVU3Hr1G085050) gene, in three *hvfea* mutants using RT-qPCR. Similar to the findings in maize [21], the *WUS*-like gene showed the increased expression in *hvfea3* and no difference in *hvfea2* plants, compared with the WT, but was down-regulated in the *hvfea4* mutant (Fig. S11B). Elucidation of the relationship between *HvFEA4* and *HvFEA2/3* or the CLV–WUS pathway must await further genetic investigations by development of higher-order mutants.

4. Discussion

4.1. IM size is negatively associated with yield traits in barley

The transforming from SAM into IM is a pivotal event in plant reproductive development [1,4]. In cereal crops, IM cells proliferate

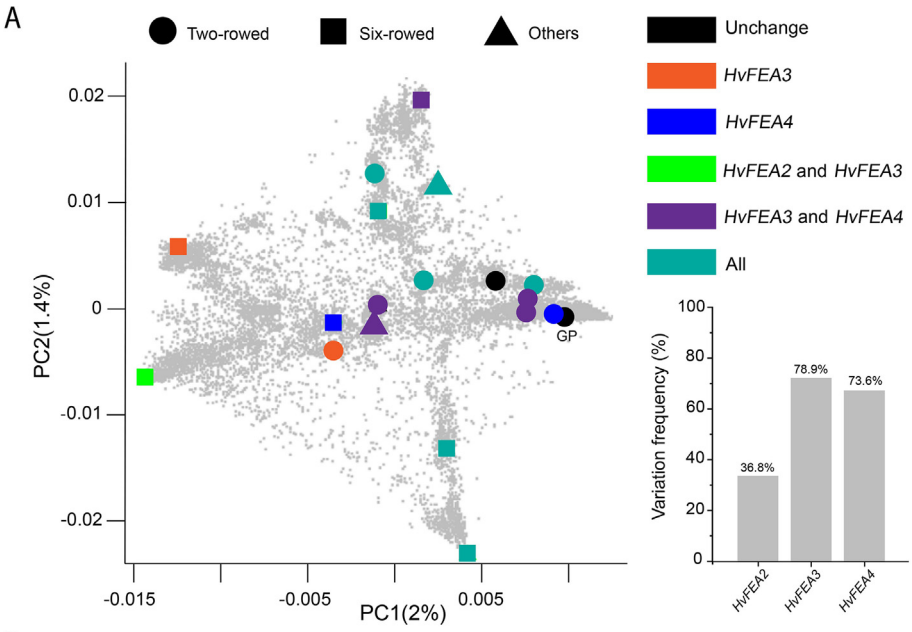

B

Variation of *HvFEA4*

Varieties	Row type	Positions and sequence variants of HvFEA4				Count	Type of mutation
		96	123	142-143	192		
Golden Promise	two-rowed	A	G	N/A	S	450	samesense
Akashinriki	six-rowed	T	D	N/A	A	450	missense
Barke	two-rowed	A	D	N/A	S	450	missense
HOR_10350	labile	A	D	N/A	S	450	missense
HOR_3365	two-rowed	A	D	N/A	S	450	missense
HOR_9043	two-rowed	A	D	N/A	S	450	missense
Hockett	two-rowed	A	D	N/A	S	450	missense
RGT_Planet	two-rowed	A	D	N/A	S	450	missense
ZDM02064	six-rowed	T	D	N/A	A	450	missense
HOR_13821	two-rowed	A	D	GT	A	452	missense and codon
HOR_21599	six-rowed	A	D	GT	A	452	missense and codon
HOR_7552	six-rowed	A	D	GT	A	452	missense and codon
HOR_8148	two-rowed	A	D	GT	A	452	missense and codon
OUN333	two-rowed	A	D	GT	A	452	missense and codon
ZDM01467	four-rowed	A	D	GT	A	452	missense and codon

Fig. 5. Natural variation of *HvFEAs* in barley. (A) Global variations of *HvFEA2*, *HvFEA3* and *HvFEA4* in 19 barley varieties that represent genetic diversity, as revealed by PCA (Principal component analysis) of genotyping-by-sequencing data of 19,778 domesticated barley varieties [56]. Principal component (PC) data of domesticated varieties originated from a pan-genome study [57]. Different shapes indicate row types (others, four-rowed, and labile). Different colors indicate whether mutations of *HvFEA2*, *HvFEA3* and *HvFEA4* have occurred between GP (Golden Promise) and other varieties. (B) Amino acid sequence alignment of HvFEA4. Only variations between GP and other varieties are shown. Numbers correspond to positions in amino acid alignment.

to generate a series of branches and/or spikelet meristems that will form kernels after fertilization [2,5]. Selection of favorable inflorescence architecture during crop breeding is key to achieving desirable production. Based on a previous hypothesis in maize [28], larger IMs provide more space around the meristem and allow the production of extra successive meristems, leading to more kernels or larger ears to reach higher yield. However, the correlation between IM size and yield traits components in barley shows the opposite trend. Barley IM width has negative effects on spikelet number, seed number, and spike length (Fig. 1). Barley varieties with large IMs tend to have unsatisfactory yield-related spike traits. We speculate that the different architecture and developmental process of inflorescence between maize and barley are the fundamental reasons for the opposite effects of IM size on yield traits. Maize yield strongly depends on the number of kernels per ear, and the IM of ears further differentiates into multiple-rowed axes bearing spikelets. Thus, wider IMs naturally have more room for extra AMs, and taller IMs develop into longer ears, eventually resulting in more kernels on each cob [21,28]. In Triticeae crops, like barley, IM directly differentiates into many spikelets arranged on both sides of the spike [4]. The wider IMs may repress spike elongation, so that more compressed space of axis limits spikelet formation.

4.2. HvFEA2, HvFEA3, and HvFEA4 are required for barley spike development and yield traits

Genetic studies have revealed regulatory genes that function in IM identification and activity and are tightly associated with yield traits of crops [4,5,11]. In maize, "fasciation" mutants with enlarged IMs have been frequently revealed to be CLV/WUS-related genes [18–21], such as TD1, FEA2 and FEA3. CLV–independent pathways have also been revealed by another maize fasciated ear mutant, with mutation of a bZIP transcription factor gene, FEA4 [23]. In this study, we identified barley HvFEA2, HvFEA3 and HvFEA4 as orthologs of maize FEA2 (also an ortholog of *Arabidopsis* CLV2), FEA3 and FEA4, respectively. These proteins exhibit high similarities in amino acid sequences and motif structures with other orthologs of grass family. Although HvFEA2 and HvFEA3 are predicted as leucine-rich repeat receptor kinases, similar to

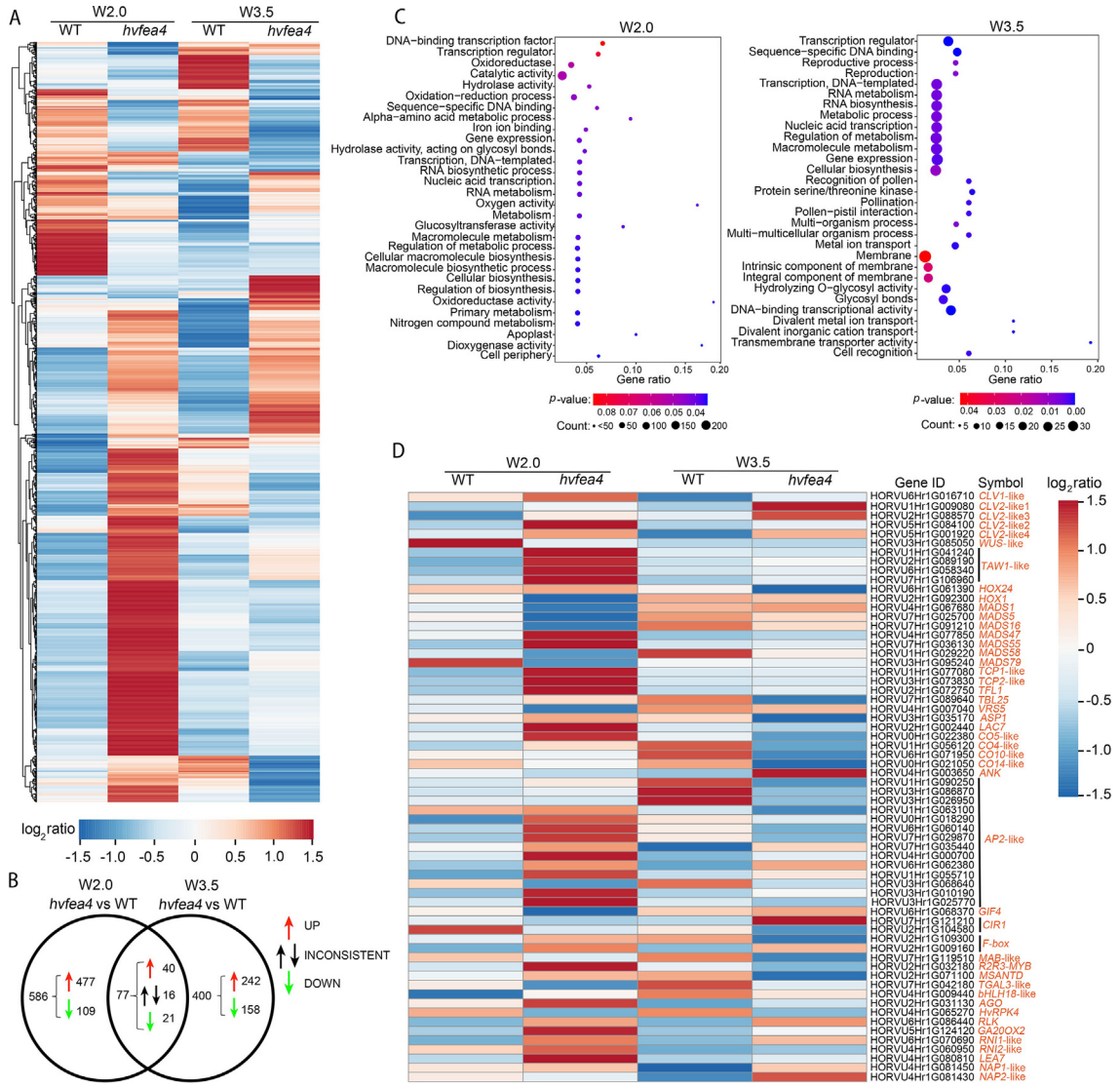

Fig. 6. HvFEA4 regulates transcriptome programming during barley inflorescence development. (A) Heatmap of expressed genes of WT and *hvfea4* mutant in spike meristem stages W2.0 and W3.5. (B) Venn diagram showing the overlap of transcripts that were differentially expressed between WT and *hvfea4* of the two spike meristem stages W2.0 and W3.5. Red arrows indicate up-regulated genes, green arrows indicate down-regulated genes, double black arrows indicate genes inconsistently regulated between the two spike meristem stages. (C) Enriched GO terms among DEGs at W2.0 and W3.5, GO terms assigned to biological processes, cellular components, and molecular function. Count number (Count) indicates the enriched gene number (circle sizes) of DEGs in each GO term. Different colors of circle indicate various values of GO enrichment (*P*-adjust). (D) Heatmap of inflorescence development-associated genes that were selected from DEGs in transcriptome sequencing. *CLV*, *CLAVATA*; *WUS*, *WUSCHEL*; *TAW*, *TAWAWA*; *HOX*, *homeobox-leucine zipper protein family*; *MADS*, *MAD-box transcription factor*; *TCP*, *Teosinte Branched1/Cincinnata/Proliferating cell factor*; *TFL*, *TERMINAL FLOWER*; *TBL*, *TRICHOME BIREFRINGENCE-LIKE*; *VRS*, *SIX-ROWED SPIKE*; *ASP*, *ABERRANT SPIKELET AND PANICLE*; *LAC*, *LACCASE*; *CO*, *CONSTANS*; *ANK*, *ANKYRIN*; *AP*, *APETALA*; *GIF*, *growth-regulating factor*; *CIR*, *CIRCADIAN*; *F-box*, *F-box protein family*; *MAB*, *BTB/POZ And MATH Domain-containing*; *R2R3-MYB*, *R2R3-MYELOBLASTOSIS transcriptional factor*; *MSANTD*, *Myb/SANT-like DNA-binding domain-containing protein*; *TGAL*, *TGA-like transcription factor*; *bHLH*, *Basic Helix-loop-Helix*; *AGO*, *Argonaute family protein*; *RPK*, *receptor-like protein kinase*; *RLK*, *receptor-like kinase*; *GA20OX2*, *gibberellin 20 Oxidase 2*; *RNI*, *RNI-like superfamily protein*; *LEA*, *late embryogenesis abundant protein*; *NAP*, *NAC domain containing protein*.

maize orthologs, they lack any kinase or other potential signaling domain [21,28] (Fig. S2A–C). Also, consistent with subcellular localizations of orthologs in maize [18,21,64], both HvFEA3 and HvFEA2 are present on the plasma membrane, although only the FEA3 family has a predicted transmembrane domain. Although most plant species have at least two members of the FEA3 and FEA4 families, only one ortholog of each has been identified in barley, indicating the evolutionary divergence of these two gene families.

We applied a monocot-optimized CRISPR/Cas9 efficient gene editing system to create *hvfea* mutants [44]. Independent alleles of *hvfea* mutants display consistent phenotypes. Commonly, *hvfea2*, *hvfea3* and *hvfea4* mutants share a similar phenotype of enlarged IM size, mimicking maize fasciated ear mutants [21,23,28]. Supporting the negative correlation between IM size and yield traits shown by 100 barley cultivars, enlarged IM of *hvfea2*, *hvfea3* and *hvfea4* mutants represses spikelet meristem formation (Fig. 3). Unlike *HvFEA2* and *HvFEA4*, transcripts of *HvFEA3* were not detected in the IM region in the early stage, suggesting that HvFEA3 may function in a non-cell-autonomous way, like the classic WUS-CLV3 loop, to control barley spike meristem development. These findings suggest that the *HvFEA2*, *HvFEA3* and *HvFEA4* genes are essential for spikelet meristem formation. The defective activity of IM in these mutants ultimately results in shorter spike length, reduced spikelet number, and reduced seed number (Fig. 4). By contrast,

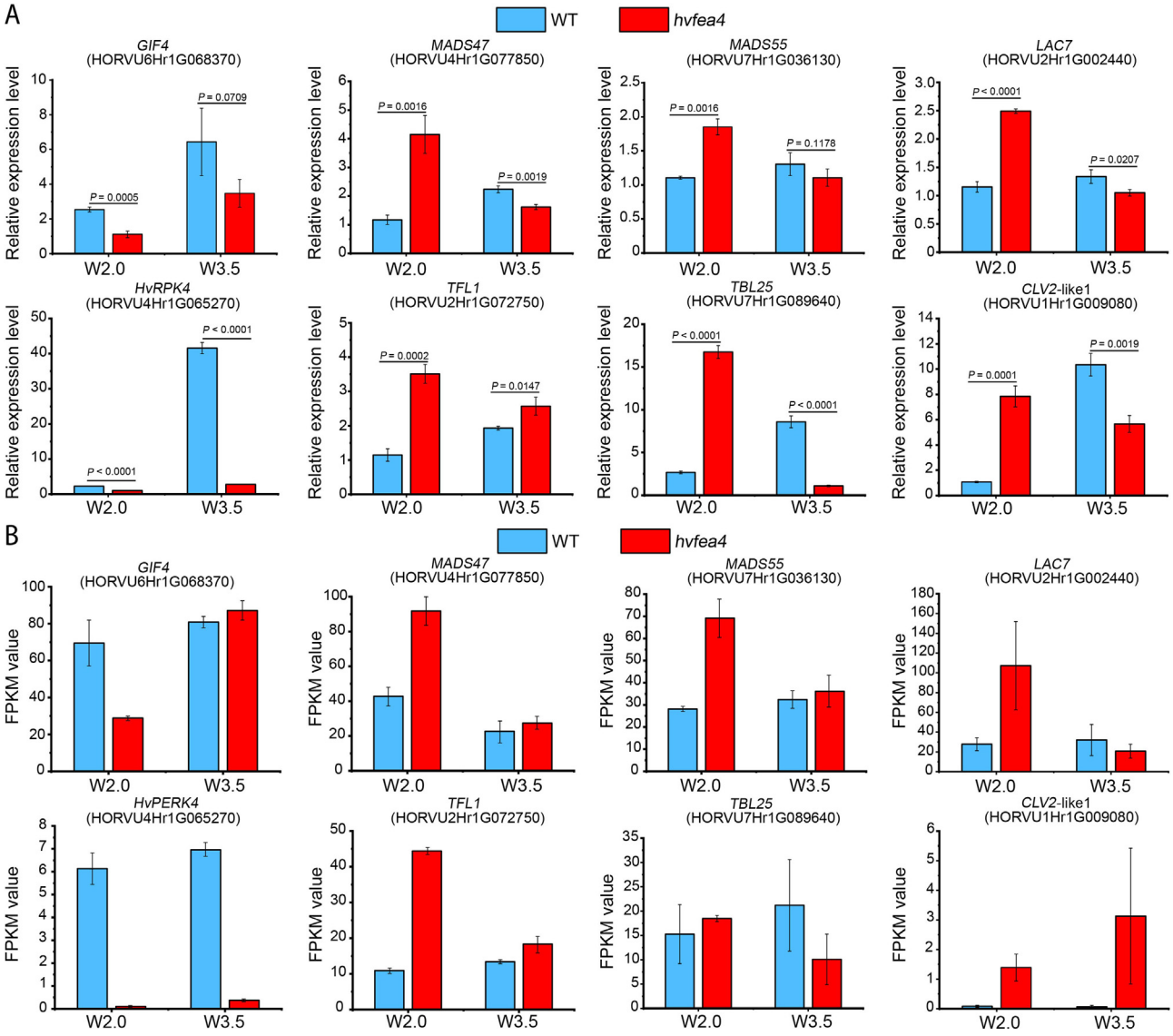

Fig. 7. Expression analysis of inflorescence development genes regulated by HvFEA4. (A) RT-qPCR analysis of significantly misregulated genes related to inflorescence development. Student's *t*-test was used for comparison (*P*-values). (B) RNA sequencing-derived expression data of selected DEGs involved in inflorescence development, mentioned in (A). The normalized expression values are reported in FPKM.

maize *fea* and rice *fon2/4* mutants, with more AMs generated from enlarged IM, develop more kernel rows in maize and more primary branches and floral organs in rice [16,21,23,28]. Barley enlarged IM mutants display reduced grain length and weight, particularly in *hvfea2* and *hvfea3* mutants, likely causing yield reduction.

The strength of CLV mutants is critical for breeding applications. Null alleles of meristem-associated genes frequently cause striking phenotypes with deleterious effects on yield traits. Maize fasciated ear mutants give rise to disorganized inflorescences with poor seed yield [19,21,23,64,65]. However, some alleles with reduced expression can increase IM size as well as kernel row number [21,28]. Recently, a weak allele of maize *FEA2* has been found that showed higher kernel row number and yield in field tests [29]. In our study, highly active variations of *HvFEAs* in barley accessions suggest their involvement in spike traits and yield during barley domestication and breeding. Therefore, breeding-favorable alleles of barley *HvFEA2*, *HvFEA3* and *HvFEA4* may be further identified in natural populations or created by CRISPR/Cas9 editing of their *cis*-elements in promoters.

4.3. HvFEA4 controls barley inflorescence development by regulating multiple biological events and signaling

Among the three *hvfea* mutants, *hvfea4* developed ectopic spikelets and the arrangement pattern of spikelets appeared opposite, but neither *hvfea2* nor *hvfea3* showed a similar phenotype in spikes (Fig. 4A, B). *HvFEA4* encodes a bZIP transcription factor, ortholog of maize FEA4 and *Arabidopsis* PERIANTHIA (PAN). Ears of the maize fea4 mutant are massively fasciated and shorter than wild-type, showing disorganized seed rows [23]. *Arabidopsis PAN* also acts as a multifunctional hub for diverse meristematic functions [66]. PAN has been demonstrated to have transcription activity only in the presence of coactivators [67]. However, the transcription activities of both HvFEA4 and maize FEA4 remain to be tested.

Our transcriptome analysis revealed that HvFEA4 functions in controlling multiple pathways and events, including inflorescence development, DNA binding, plant hormone signaling, and redox status homeostasis. Most of the DEGs that control these processes were up-regulated in *hvfea4* mutants, suggesting that HvFEA4 may act as a transcriptional repressor of its targets. In particular, auxin

response genes and oxidation-associated genes were generally up-regulated at early stages of *hvfea4* meristems, and our PPI also revealed the redox network among up-regulated DEGs. Thus, HvFEA4 appears to inhibit auxin response and prevent excessive redox response in barley spike meristems. However, maize FEA4 functions in activating auxin pathway genes, and *Arabidopsis* PAN is also able to modulate auxin dependent developmental events [23,66], suggesting divergent functions of FEA4 orthologs. The detailed mechanisms by which bZIP transcription factor regulates auxin signaling remain unknown. Notably, maize FEA4 interacts with glutaredoxins (GRXs) that are small oxidoreductases, and GRXs also regulate the redox state and transcriptional activities of FEA4 to control inflorescence development [24,25], suggesting that redox signaling may function in plant inflorescence development via interactions with FEA4. Even though several oxidation reaction genes are likely regulated by HvFEA4, the relationship between redox status control and HvFEA4 awaits elucidation.

HvFEA4 also directly or indirectly maintains the expression of some key inflorescence genes, like *VRS5* and *HvMADS1* [33,37]. The PPI of down-regulated DEGs shows the network linking HvFEA4 and MADS proteins. HvFEA4 may influence some downstream genes in common with barley HvMADS1; *RPK4* (*Receptor-like Protein Kinase*, HORVU4Hr1G065270) shows greatly reduced expression both in *hvfea4* and *hvmads1* mutants [37]. These results shed light on the crosstalk between HvFEA4 and other regulators.

In summary, our results reveal a negative trend between IM size and yield traits in barley spikes, in contrast to those of previous studies of other major cereals, likely owing to their differentiated inflorescence architectures and progressions. CLV orthologs, HvFEA2 and HvFEA3, and bZIP transcription factor HvFEA4, function as key regulators controlling barley IM size, spike architecture, and yield traits. Our study also explores the molecular regulatory network of HvFEA4, uncovering key biological events affected by HvFEA4 during barley spike development. Together, our findings highlight the novelty of IM-size-inhibited yield traits in barley and suggest the complexity of orthologous genes' functions in different species, extending our understanding of how the meristem affects grain yield and facilitating crop improvement.

CRediT authorship contribution statement

Chengyu Wang: Writing – original draft, Data curation, Investigation, Formal analysis. **Xiujunan Yang:** Writing – review & editing, Investigation, Resources. **Yueya Zhang:** Investigation, Resources, Data curation. **Chaoqun Shen:** Investigation, Resources, Data curation. **Jin Shi:** Investigation, Resources, Data curation. **Chongjing Xia:** Data curation. **Taohong Fang:** Investigation, Resources, Data curation. **Qiang Tu:** Investigation, Resources, Data curation. **Ling Li:** Investigation, Resources, Data curation. **Xinli Zhou:** Data curation. **Dabing Zhang:** Data curation. **Gang Li:** Conceptualization, Project administration, Writing – review & editing.

Declaration of competing interest

The authors declare that they have no known competing financial interests or personal relationships that could have appeared to influence the work reported in this paper.

Acknowledgments

This work was financially supported by the Science and Research Grant of Southwest University of Science and Technology (19zx7146), the start-up grant from Nanjing Agricultural University (to Gang Li), the Australia–China Science and Research Fund Joint Research Centre grant (ACSRF48187), the Australian Research Council (DP170103352), and the Waite Research Institute (WRI) of the University of Adelaide. We thank prof. Yaoguang Liu (South China Agricultural University) for providing vectors pYLsgRNA–OsU6a, pYLsgRNA–OsU6b and pYLCRISPR–Cas9Pubi–H for CRISPR/Cas9 editing. We thank Dr. Gwen Mayo (Adelaide Microscopy) for assistance in the microscopy work, and Miss Hui Zhou (University of Adelaide) for managing the plant materials.

Appendix A. Supplementary data

Supplementary data for this article can be found online at https://doi.org/10.1016/j.cj.2022.10.001.

References

[1] B. Wang, S.M. Smith, J. Li, Genetic regulation of shoot architecture, Annu. Rev. Plant Biol. 69 (2018) 437–468.
[2] P. Bommert, C. Whipple, Grass inflorescence architecture and meristem determinacy, Semin. Cell Dev. Biol. 79 (2018) 37–44.
[3] S. Sakuma, T. Schnurbusch, Of floral fortune: tinkering with the grain yield potential of cereal crops, New Phytol. 225 (2020) 1873–1882.
[4] C. Wang, X. Yang, G. Li, Molecular insights into inflorescence meristem specification for yield potential in cereal crops, Int. J. Mol. Med. 22 (2021) 3508.
[5] D. Zhang, Z. Yuan, Molecular control of grass inflorescence development, Annu. Rev. Phytopathol. 65 (2014) 553–578.
[6] S. Li, S. Meng, J. Weng, Q. Wu, Fine-tuning shoot meristem size to feed the world, Trends Plant Sci. 27 (2022) 355–363.
[7] H. Schoof, M. Lenhard, A. Haecker, K.F.X. Mayer, G. Jürgens, T. Laux, The stem cell population of *Arabidopsis* shoot meristems in maintained by a regulatory loop between the *CLAVATA* and *WUSCHEL* genes, Cell 100 (2000) 635–644.
[8] K. Miyawaki, R. Tabata, S. Sawa, Evolutionarily conserved CLE peptide signaling in plant development, symbiosis, and parasitism, Curr. Plant Biol. 16 (2013) 598–606.
[9] M. Somssich, B.I. Je, R. Simon, D. Jackson, CLAVATA-WUSCHEL signaling in the shoot meristem, Development 143 (2016) 3238–3248.
[10] J.C. Fletcher, The CLV-WUS stem cell signaling pathway: a roadmap to crop yield optimization, Plants 7 (2018) 87.
[11] M. Kitagawa, D. Jackson, Control of meristem size, Annu. Rev. Phytopathol. 70 (2019) 269–291.
[12] S.E. Clark, R.W. Williams, E.M. Meyerowitz, The *CLAVATA1* gene encodes a putative receptor kinase that controls shoot and floral meristem size in *Arabidopsis*, Cell 89 (1997) 575–585.
[13] J.C. Fletcher, U. Brand, M.P. Running, R. Simon, E.M. Meyerowitz, Signaling of cell fate decisions by *CLAVATA3* in *Arabidopsis* shoot meristems, Science 283 (1999) 1911–1914.
[14] S. Jeong, A.E. Trotochaud, S.E. Clark, The *Arabidopsis CLAVATA2* gene encodes a receptor-like protein required for the stability of the CLAVATA1 receptor-like kinase, Plant Cell 11 (1999) 1925–1933.
[15] T. Suzaki, M. Sato, M. Ashikari, M. Miyoshi, Y. Nagato, H.Y. Hirano, The gene *FLORAL ORGAN NUMBER1* regulates floral meristem size in rice and encodes a leucine-rich repeat receptor kinase orthologous to *Arabidopsis* CLAVATA1, Development 131 (2004) 5649–5657.
[16] T. Suzaki, T. Toriba, M. Fujimoto, N. Tsutsumi, H. Kitano, H.Y. Hirano, Conservation and diversification of meristem maintenance mechanism in *Oryza sativa*: function of the *FLORAL ORGAN NUMBER2* gene, Plant Cell Physiol. 47 (2006) 1591–1602.
[17] H. Chu, Q. Qian, W. Liang, C. Yin, H. Tan, X. Yao, Z. Yuan, J. Yang, H. Huang, D. Luo, H. Ma, D. Zhang, The *FLORAL ORGAN NUMBER4* gene encoding a putative ortholog of *Arabidopsis* CLAVATA3 regulates apical meristem size in rice, Plant Physiol. 142 (2006) 1039–1052.
[18] F. Taguchi-Shiobara, Z. Yuan, S. Hake, D. Jackson, The *FASCIATED EAR2* gene encodes a leucine-rich repeat receptor-like protein that regulates shoot meristem proliferation in maize, Genes Dev. 15 (2001) 2755–2766.
[19] P. Bommert, C. Lunde, J. Nardmann, E. Vollbrecht, M. Running, D. Jackson, S. Hake, W. Werr, *Thick tassel dwarf1* encodes a putative maize ortholog of the *Arabidopsis CLAVATA1* leucine-rich repeat receptor-like kinase, Development 132 (2005) 1235–1245.
[20] B.I. Je, F. Xu, Q. Wu, L. Liu, R. Meeley, J.P. Gallagher, L. Corcilius, R.J. Payne, M.E. Bartlett, D. Jackson, The CLAVATA receptor FASCIATED EAR2 responds to distinct CLE peptides by signaling through two downstream effectors, Elife 7 (2018) e35673.
[21] B.I. Je, J. Gruel, Y.K. Lee, P. Bommert, E.D. Arevalo, A.L. Eveland, Q. Wu, A. Goldshmidt, R. Meeley, M. Bartlett, M. Komatsu, H. Sakai, H. Jönsson, D. Jackson, Signaling from maize organ primordia via FASCIATED EAR3 regulates stem cell proliferation and yield traits, Nat. Genet. 48 (2016) 785–791.
[22] Z. Chen, A. Gallavotti, Improving architectural traits of maize inflorescences, Mol. Breed. 41 (2021) 21.
[23] M. Pautler, A.L. Eveland, T. LaRue, F. Yang, R. Weeks, C. Lunde, B.I. Je, R. Meeley, M. Komatsu, E. Vollbrecht, H. Sakai, D. Jackson, *FASCIATED EAR4* encodes a bZIP transcription factor that regulates shoot meristem size in maize, Plant Cell 27 (2015) 104–120.

[24] F. Yang, H.T. Bui, M. Pautler, V. Llaca, R. Johnston, B.H. Lee, A. Kolbe, H. Sakai, D. Jackson, A maize glutaredoxin gene, *Abphy12*, regulates shoot meristem size and phyllotaxy, Plant Cell 27 (2015) 121–131.
[25] R.S. Yang, F. Xu, Y.M. Wang, W.S. Zhong, L. Dong, Y.N. Shi, T.J. Tang, H.J. Sheng, D. Jackson, F. Yang, Glutaredoxins regulate maize inflorescence meristem development via redox control of TGA transcriptional activity, Nat. Plants 7 (2021) 1589–1601.
[26] C. Xu, K.L. Liberatore, C.A. MacAlister, Z. Huang, Y.H. Chu, K.E. Jiang, C. Brooks, M. Ogawa-Ohnishi, G. Xiong, M. Pauly, J. Van Eck, Y. Matsubayashi, E. van der Knaap, Z.B. Lippman, A cascade of arabinosyltransferases controls shoot meristem size in tomato, Nat. Genet. 47 (2015) 784–792.
[27] D. Rodriguez-Leal, C. Xu, C.T. Kwon, C. Soyars, E. Demesa-Arevalo, J. Man, L. Liu, Z.H. Lemmon, D.S. Jones, J. Van Eck, D.P. Jackson, M.E. Bartlett, Z.L. Nimchuk, Z. B. Lippman, Evolution of buffering in a genetic circuit controlling plant stem cell proliferation, Nat. Genet. 51 (2019) 786–792.
[28] P. Bommert, N.S. Nagasawa, D. Jackson, Quantitative variation in maize kernel row number is controlled by the *FASCIATED EAR2* locus, Nat. Genet. 45 (2013) 334–337.
[29] K.H. Trung, Q.H. Tran, N.H. Bui, T.T. Tran, K.Q. Luu, N.T.T. Tran, L.T. Nguyen, D.T. N. Nguyen, N.D. Vu, D.T.T. Quan, D.T. Nguyen, H.T. Nguyen, C.C. Dang, B.M. Tran, T.D. Khanh, S.L. Vi, A weak allele of *FASCIATED EAR 2* (*FEA*2) increases maize kernel row number (KRN) and yield in elite maize hybrids, Agronomy 10 (2020) 1774.
[30] D. Rodríguez-Leal, Z.H. Lemmon, J. Man, M.E. Bartlett, Z.B. Lippman, Engineering quantitative trait variation for crop improvement by genome editing, Cell 171 (2017) 470–480.
[31] L. Liu, J. Gallagher, E.D. Arevalo, R. Chen, T. Skopelitis, Q. Wu, M. Bartlett, D. Jackson, Enhancing grain-yield-related traits by CRISPR-Cas9 promoter editing of maize *CLE* genes, Nat. Plants 7 (2021) 287–294.
[32] X.Q. Gao, N. Wang, X.L. Wang, X.S. Zhang, Architecture of wheat inflorescence: insights from rice, Trends Plant Sci. 24 (2019) 802–809.
[33] L. Ramsay, J. Comadran, A. Druka, D.F. Marshall, W.T.B. Thomas, M. Macaulay, K. MacKenzie, C. Simpson, J. Fuller, N. Bonar, P.M. Hayes, U. Lundqvist, J.D. Franckowiak, T.J. Close, G.J. Muehlbauer, R. Waugh, *INTERMEDIUM-C*, a modifier of lateral spikelet fertility in barley, is an ortholog of the maize domestication gene *TEOSINTE BRANCHED 1*, Nat. Genet. 43 (2011) 169–172.
[34] N. Poursarebani, T. Seidensticker, R. Koppolu, C. Trautewig, P. Gawroński, F. Bini, G. Govind, T. Rutten, S. Sakuma, A. Tagiri, G.M. Wolde, H.M. Youssef, A. Battal, S. Ciannamea, T. Fusca, T. Nussbaumer, C. Pozzi, A. Börner, U. Lundqvist, T. Komatsuda, S. Salvi, R. Tuberosa, C. Uauy, N. Sreenivasulu, L. Rossini, T. Schnurbusch, The genetic basis of composite spike form in barley and 'Miracle-Wheat', Genetics 201 (2015) 155–165.
[35] J.M. Debernardi, J.R. Greenwood, E.J. Finnegan, J. Jernstedt, J. Dubcovsky, *APETALA 2*-like genes *AP2L2* and *Q* specify lemma identity and axillary floral meristem development in wheat, Plant J. 101 (2019) 171–187.
[36] Y.I. Shang, L.U. Yuan, Z. Di, Y. Jia, Z. Zhang, S. Li, L. Xing, Z. Qi, X. Wang, J. Zhu, W. Hua, X. Wu, M. Zhu, G. Li, C. Li, F. Wellmer, A CYC/TB1-type TCP transcription factor controls spikelet meristem identity in barley, J. Exp. Bot. 71 (2020) 7118–7131.
[37] G. Li, H.N.J. Kuijer, X. Yang, H. Liu, C. Shen, J. Shi, N. Betts, M.R. Tucker, W. Liang, R. Waugh, R.A. Burton, D. Zhang, MADS1 maintains barley spike morphology at high ambient temperatures, Nat. Plants 7 (2021) 1093–1107.
[38] K. Li, J.M. Debernardi, C. Li, H. Lin, C. Zhang, J. Jernstedt, M.V. Korff, J. Zhong, J. Dubcovsky, Interactions between SQUAMOSA and SHORT VEGETATIVE PHASE MADS-box proteins regulate meristem transitions during wheat spike development, Plant Cell 33 (2021) 3621–3644.
[39] H.N. Kuijer, N.J. Shirley, S.F. Khor, J. Shi, J. Schwerdt, D. Zhang, G. Li, R.A. Burton, Transcript profiling of MIKCc MADS-Box genes reveals conserved and novel roles in barley inflorescence development, Front. Plant Sci. 12 (2021).
[40] H. Liu, G. Li, X. Yang, H.N.J. Kuijer, W. Liang, D. Zhang, Transcriptome profiling reveals phase-specific gene expression in the developing barley inflorescence, Crop J. 8 (2020) 71–86.
[41] M. Mascher, H. Gundlach, A. Himmelbach, S. Beier, S.O. Twardziok, T. Wicker, V. Radchuk, C. Dockter, P.E. Hedley, J. Russell, M. Bayer, L. Ramsay, H. Liu, G. Haberer, X.Q. Zhang, Q. Zhang, R.A. Barrero, L. Li, S. Taudien, M. Groth, M. Felder, A. Hastie, H. Šimková, H. Staňková, J. Vrána, S. Chan, M. Muñoz-Amatriaín, R. Ounit, S. Wanamaker, D. Bolser, C. Colmsee, T. Schmutzer, L. Aliyeva-Schnorr, S. Grasso, J. Tanskanen, A. Chailyan, D. Sampath, D. Heavens, L. Clissold, S. Cao, B. Chapman, F. Dai, Y. Han, H. Li, X. Li, C. Lin, J.K. McCooke, C. Tan, P. Wang, S. Wang, S. Yin, G. Zhou, J.A. Poland, M.I. Bellgard, L. Borisjuk, A. Houben, J. Doležel, S. Ayling, S. Lonardi, P. Kersey, P. Langridge, G.J. Muehlbauer, M.D. Clark, M. Caccamo, A.H. Schulman, K.F.X. Mayer, M. Platzer, T.J. Close, U. Scholz, M. Hansson, G. Zhang, I. Braumann, M. Spannagl, C. Li, R. Waugh, N. Stein, A chromosome conformation capture ordered sequence of the barley genome, Nature 544 (2017) 427–433.
[42] R. Bouckaert, J. Heled, D. Kuhnert, T. Vaughan, C.H. Wu, D. Xie, M.A. Suchard, A. Rambaut, A.J. Drummond, BEAST 2: a software platform for bayesian evolutionary analysis, PLoS Comput. Biol. 10 (2014) e1003537.
[43] G.C. Yu, D.K. Smith, H.C. Zhu, Y. Guan, T.T.Y. Lam, GGTREE: an R package for visualization and annotation of phylogenetic trees with their covariates and other associated data, Methods Ecol. Evol. 8 (2017) 28–36.
[44] X. Ma, Q. Zhang, Q. Zhu, W. Liu, Y. Chen, R. Qiu, B. Wang, Z. Yang, H. Li, Y. Lin, Y. Xie, R. Shen, S. Chen, Z. Wang, Y. Chen, J. Guo, L. Chen, X. Zhao, Z. Dong, Y.G. Liu, A robust CRISPR/Cas9 system for convenient, high-efficiency multiplex genome editing in monocot and dicot plants, Mol. Plant 8 (2015) 1274–1284.
[45] W.A. Harwood, J.G. Bartlett, S.C. Alves, M. Perry, M.A. Smedley, N. Leyland, J.W. Snape, Barley transformation using *Agrobacterium*-mediated techniques, Methods Mol. Biol. 478 (2009) 137–147.
[46] B. Digel, A. Pankin, M. von Korff, Global transcriptome profiling of developing leaf and shoot apices reveals distinct genetic and environmental control of floral transition and inflorescence development in barley, Plant Cell 27 (2015) 2318–2334.
[47] N. Satoh-Nagasawa, N. Nagasawa, S. Malcomber, H. Sakai, D. Jackson, A trehalose metabolic enzyme controls inflorescence architecture in maize, Nature 441 (2006) 227–230.
[48] X. Yang, G. Li, Y. Tian, Y. Song, W. Liang, D. Zhang, A rice glutamyl-tRNA synthetase modulates early anther cell division and patterning, Plant Physiol. 177 (2018) 728–744.
[49] G. Li, W. Liang, X. Zhang, H. Ren, J. Hu, M.J. Bennett, D. Zhang, Rice actin-binding protein RMD is a key link in the auxin-actin regulatory loop that controls cell growth, Proc. Natl. Acad. Sci. U. S. A. 111 (2014) 10377–10382.
[50] H. Li, B. Handsaker, A. Wysoker, T. Fennell, J. Ruan, N. Homer, G. Marth, G. Abecasis, R. Durbin, The sequence alignment/map format and SAMtools, Bioinformatics 25 (2009) 2078–2079.
[51] F. Ramírez, D.P. Ryan, B. Grüning, V. Bhardwaj, F. Kilpert, A.S. Richter, S. Heyne, F. Dündar, T. Manke, DeepTools2: a next generation web server for deep-sequencing data analysis, Nucleic Acids Res. 44 (2016) 160–165.
[52] G. Csaba, E. Berchtold, A. Hadziahmetovic, M. Gruber, C. Ammar, R. Zimmer, Empires: differential analysis of gene expression and alternative splicing, bioRxiv (2020), https://doi.org/10.1101/2020.08.23.234237.
[53] Y. Zhou, B. Zhou, L. Pache, M. Chang, A.H. Khodabakhshi, O. Tanaseichuk, C. Benner, S.K. Chanda, Metascape provides a biologist-oriented resource for the analysis of systems-level datasets, Nat. Commun. 10 (2019) 1523.
[54] S. Ma, S. Sun, L. Geng, M. Song, W. Wang, Y. Ye, Q. Ji, Z. Zou, S.I. Wang, X. He, W. Li, C.R. Esteban, X. Long, G. Guo, P. Chan, Q.I. Zhou, J.C.I. Belmonte, W. Zhang, J. Qu, G.H. Liu, Caloric restriction reprograms the single-cell transcriptional landscape of *Rattus norvegicus* aging, Cell 180 (2020) 984–1001.
[55] M.E. Smoot, K. Ono, J. Ruscheinski, P.L. Wang, T. Ideker, Cytoscape 2.8: new features for data integration and network visualization, Bioinformatics 27 (2011) 431–432.
[56] S.G. Milner, M. Jost, S. Taketa, E.R. Mazón, A. Himmelbach, M. Oppermann, S. Weise, H. Knüpffer, M. Basterrechea, P. König, D. Schüler, R. Sharma, R.K. Pasam, T. Rutten, G. Guo, D. Xu, J. Zhang, G. Herren, T. Müller, S.G. Krattinger, B. Keller, Y. Jiang, M.Y. González, Y. Zhao, A. Habekuß, S. Färber, F. Ordon, M. Lange, A. Börner, A. Graner, J.C. Reif, U. Scholz, M. Mascher, N. Stein, Genebank genomics highlights the diversity of a global barley collection, Nat. Genet. 51 (2019) 319–326.
[57] M. Jayakodi, S. Padmarasu, G. Haberer, V.S. Bonthala, H. Gundlach, C. Monat, T. Lux, N. Kamal, D. Lang, A. Himmelbach, J. Ens, X.Q. Zhang, T.T. Angessa, G. Zhou, C. Tan, C. Hill, P. Wang, M. Schreiber, L.B. Boston, C. Plott, J. Jenkins, Y.U. Guo, A. Fiebig, H. Budak, D. Xu, J. Zhang, C. Wang, J. Grimwood, J. Schmutz, G. Guo, G. Zhang, K. Mochida, T. Hirayama, K. Sato, K.J. Chalmers, P. Langridge, R. Waugh, C.J. Pozniak, U. Scholz, K.F.X. Mayer, M. Spannagl, C. Li, M. Mascher, N. Stein, The barley pan-genome reveals the hidden legacy of mutation breeding, Nature 588 (2020) 284–289.
[58] S.R. Waddington, P.M. Cartwright, P.C. Wall, A quantitative scale of spike initial and pistil development in barley and wheat, Ann. Bot. 51 (1983) 119–130.
[59] A. Yoshida, M. Sasao, N. Yasuno, K. Takagi, Y. Daimon, R. Chen, R. Yamazaki, H. Tokunaga, Y. Kitaguchi, Y. Sato, Y. Nagamura, T. Ushijima, T. Kumamaru, S. Iida, M. Maekawa, J. Kyozuka, *TAWAWA1*, a regulator of rice inflorescence architecture, functions through the suppression of meristem phase transition, Proc. Natl. Acad. Sci. U. S. A. 110 (2013) 767–772.
[60] A. Yoshida, Y. Ohmori, H. Kitano, F. Taguchi-Shiobara, H.Y. Hirano, *ABERRANT SPIKELET AND PANICLE1*, encoding a TOPLESS-related transcriptional co-repressor, is involved in the regulation of meristem fate in rice, Plant J. 70 (2012) 327–339.
[61] H.M. Youssef, K. Eggert, R. Koppolu, A.M. Alqudah, N. Poursarebani, A. Fazeli, S. Sakuma, A. Tagiri, T. Rutten, G. Govind, U. Lundqvist, A. Graner, T. Komatsuda, N. Sreenivasulu, T. Schnurbusch, VRS2 regulates hormone-mediated inflorescence patterning in barley, Nat. Genet. 49 (2017) 157–161.
[62] H. Asard, R. Barbaro, P. Trost, A. Bérczi, Cytochromes b561: ascorbate-mediated trans-membrane electron transport, Antioxid. Redox Signal. 19 (2013) 1026–1035.
[63] T. Nomura, T. Kushiro, T. Yokota, Y. Kamiya, G.J. Bishop, S. Yamaguchi, The last reaction producing brassinolide is catalyzed by cytochrome p-450s, CYP85A3 in tomato and CYP85A2 in *Arabidopsis*, J. Biol. Chem. 280 (2005) 17873–17879.
[64] P. Bommert, B. Je, A. Glodshmidt, D. Jackson, The maize G alpha gene *COMPACT PLANT2* functions in CLAVATA signalling to control shoot meristem size, Nature 502 (2013) 555–558.
[65] Q. Wu, F. Xu, L. Liu, S.N. Char, Y. Ding, E. Schmelz, B. Yang, D. Jackson, The maize heterotrimeric G protein beta subunit controls shoot meristem development and immune responses, Proc. Natl. Acad. Sci. U. S. A. 117 (2020) 1799–1805.
[66] J. Lohmann, A. Maier, S. Stehling-Sun, S.L. Offenburger, The bZIP transcription factor PERIANTHIA: a multifunctional hub for meristem control, Front. Plant Sci. 2 (2011) 79.
[67] A.T. Maier, S. Stehling-Sun, H. Wollmann, M. Demar, R.L. Hong, S. Haubeiss, D. Weigel, J.U. Lohmann, Dual roles of the bZIP transcription factor PERIANTHIA in the control of floral architecture and homeotic gene expression, Development 136 (2009) 1613–1620.